XANES study of rhenium oxide compounds at the L1 and L3 absorption edges

Asma Tougerti, Sylvain Cristol, Elise Berrier, Valérie Briois, Camille La Fontaine, Françoise Villain, Yves Joly

XANES study of rhenium oxide compounds at the L_1 and L_3 absorption edges

Asma Tougerti,[1,2] Sylvain Cristol,[2] Elise Berrier,[2] Valérie Briois,[3] Camille La Fontaine,[3] Françoise Villain,[3] and Yves Joly[1]

[1]*Institut Néel, CNRS & Université Joseph Fourier, Boîte Postale 166, F-38042 Grenoble Cedex 9, France*

[2]*Unité de Catalyse et de Chimie du Solide, UMR CNRS 8181, Université Lille 1, Bâtiment C3, Cité Scientifique, F-59650 Villeneuve d'Ascq, France*

[3]*Synchrotron Soleil, L'Orme des Merisiers Saint Aubin, Boîte Postale 48, F-91192 Gif sur Yvette, France*

(Received 7 April 2011; revised manuscript received 8 February 2012; published 30 March 2012)

We report on the study of a set of rhenium oxide reference compounds (NH_4ReO_4, $NaReO_4$, ReO_3, ReO_2, and Re_2O_7) using x-ray-absorption near-edge structure. The parallel use of Re L_1 and L_3 absorption edges permits a concomitant understanding of both the oxidation state and the local symmetry for these compounds. Experiments are compared with *ab initio* simulations. A good agreement is reached in most cases. The choice of the cluster size and the calculation method (full potential or not), which are mandatory ingredients allowing a satisfactory reproduction of the recorded spectra, is discussed in detail. In the meantime, these parameters give important pieces of information on the studied materials.

DOI: 10.1103/PhysRevB.85.125136 PACS number(s): 78.20.Bh, 61.05.cj

I. INTRODUCTION

Because of the remarkable activity of alumina-supported rhenium oxide catalysts in the metathesis reaction, several comprehensive studies based on structural characterization were reported in the late 1980s.[1] More recently, rhenium oxides were also identified as highly efficient catalysts for the direct conversion of methanol to dimethoxymethane (DMM): $CH_2(OCH_3)_2$.[2] Receiving a fast-growing amount of attention as an elegant way of producing chemical intermediates from biomass, this reaction requires a combination of at least one redox couple and one acidic function.[3] Rhenium oxide compounds present the right balance between these two functions to yield DMM directly from methanol. However, their efficiency still needs to be improved.

Most rhenium-based catalysts are supported or mixed with other oxides. A typical preparation consists in impregnating a given support with an aqueous solution of perrhenic acid ($HReO_4$). The solid is then subjected to a drying step followed by a heat treatment up to 400–500 °C to stabilize the oxorhenate phase. Under ambient conditions, the surface rhenium oxide species are fully hydrated monomers exhibiting a tetrahedral coordination, ReO_4, as found in perrhenic acid. Upon dehydration, the structure of the supported Re oxide is modified and is reported to depend on the nature of the support,[4,5] the preparation technique,[6,7] and the Re loading.[8] During the catalytic reaction, rhenium species can exhibit several oxidation states, different hydration degrees, and various structures.[9] As an example, the supported phase has been reported to form polymeric species such as ReO_2 (Re/α-Fe_2O_3).[2] The identification of the active phase and the depiction of the reaction mechanism can thus become quite complex. In order to precisely identify those various Re forms, a comprehensive study of reference rhenium oxide compounds is mandatory.

X-ray-absorption near-edge structure (XANES) is the part of the x-ray-absorption spectrum near the ionization threshold of core electrons with orbital momentum l belonging to the absorbing atom. This special region is sensitive to both the electronic structure of the detected absorbing atom, since the intensity of structures is nearly proportional to the density of the unoccupied states of symmetry verifying the electric dipolar selection rule $\Delta l = \pm 1$, but also to the stereochemical arrangement of neighbors around the absorbing atom.[10]

The L_1 and L_3 edges probe different orbital states ($l = 2$ for L_3 and $l = 1$ for L_1) and thus exhibit different sensitivities. A combined study of both edges can give additional pieces of information. However, one of the goals of this paper is to show a systematic comparison of the L_1 and L_3 edges for a series of compounds of the same family, and to show for a general purpose what can be obtained in this way. To obtain such results, it is often mandatory to model the experimental spectra using *ab initio* or *nearly ab initio* approaches; by *nearly* we mean that some parameters can remain adjustable in order to force evolution in the simulated spectra and to have a better understanding of the typical features observed in the experiments. In this paper, we compare a series of experimental spectra of rhenium oxides with simulated ones. Attention will be paid to the relative sensitivity of the L_1 and L_3 absorption edges. Bulk rhenium oxides were selected according to their relevance in reproducing the different Re species present in the supported Re catalysts: $NaReO_4$, NH_4ReO_4, ReO_3, ReO_2, and Re_2O_7. In the next section, we briefly present the different Re compounds. In Sec. III, sample preparation details and measurements parameters are exposed. Section IV gives some pieces of information on the theoretical part. Results are then presented in Sec. V, with a discussion on the relative sensitivity of both edges on structure and oxidation state.

II. RHENIUM OXIDE COMPOUNDS

NH_4ReO_4 is tetragonal, its space group is $I41/a$, and the unit-cell parameters are $a = b = 5.995$ Å, $c = 12.440$ Å, and $\alpha = \beta = \gamma = 90°$. The Re cation is tetrahedrally coordinated by four oxygen atoms to form the ReO_4^- anion, while NH_4^+ acts as a counterion to ensure the neutrality of the system.[11] The oxidation number of the Re atom is 7, which corresponds to a formal electronic configuration: [Xe] $4f^{14}5d^0$. $NaReO_4$ crystallizes in the same tetragonal structure with the same space group.[11] Because of the smaller size of the countercation, the unit-cell parameters are significantly smaller:

$a = b = 5.3654$ Å and $c = 11.732$ Å. Both the local structure and the oxidation number of the rhenium atom are the same as in NH_4ReO_4.

ReO_2 is orthorhombic, its space group is $Pbcn$, and the unit-cell parameters are $a = 4.8094$ Å, $b = 5.6433$ Å, $c = 4.6007$ Å, and $\alpha = \beta = \gamma = 90°$.[12] The structure can be visualized as a distorted rutile structure where the Re is octahedrally coordinated by six oxygen atoms and each oxygen atom is coordinated to three different Re cations. The ReO_6 units are linked to each other through corners and edges. The oxidation number of the Re is 4, which corresponds to an electronic configuration [Xe] $4f^{14}5d^3$.

ReO_3 is cubic, its space group is Im-3, and the unit-cell parameters are $a = b = c = 7.46$ Å and $\alpha = \beta = \gamma = 90°$.[13] The structure is made up of corner-sharing ReO_6 units. The electronic configuration of the Re atom is [Xe] $4f^{14}5d^1$ and its oxidation number is 6.

The Re_2O_7 is orthorhombic, its space group is $P2_12_12_1$, and the unit-cell parameters are $a = 12.508$ Å, $b = 15.196$ Å, $c = 5.448$ Å, and $\alpha = \beta = \gamma = 90°$.[14] The structure is made up of ReO_6 and ReO_4 units linked together by oxygen bridges to form a chain structure of double layers.

III. EXPERIMENTS

A. Sample preparation

Polycrystalline ReO_2 (99.9% purity), Re_2O_7 (99.9% purity), and ReO_3 (99.9% purity) were purchased from Alfa Æsar. Those oxides were thoughtfully ground, diluted in alumina to get a suitable absorption, and pressed into pellets. The disks were subsequently mounted in a sample holder loaded within an argon-filled glove box into an air-tight box equipped with Kapton windows to allow x-Ray transmission. To ensure a good transmission at the L_1 and L_3 Re edges, the air-tight box was continuously pumped under primary vacuum during the data acquisition. Conversely, ammonium perrhenate NH_4ReO_4 (99+%, Alfa Æsar) and sodium perrhenate $NaReO_4$ (99.99%, Aldrich) are stable under ambient conditions. After due dilution in cellulose, both samples were pressed into pellets and analyzed under ambient conditions.

B. X-ray-absorption near-edge structure measurements

The experimental XANES spectra were recorded at SOLEIL Synchrotron on the SAMBA (Spectroscopies Applied to Materials Based on Absorption) beamline.[15] The radiation from the bending magnet source was collimated by a first cylindrical bent mirror onto the Si(220) fixed exit sagitally focusing double-crystal monochromator. A second cylindrical bent mirror focused the monochromatic beam at the sample position onto a spot of 300×300 μm^2. The x-ray grazing incidence of the mirrors was set at 4 mrad in order to reject harmonics. Re L_1- and L_3-edge spectra were collected in transmission mode at room temperature, and Oxford ionization chambers were used to measure the incident and transmitted intensities.

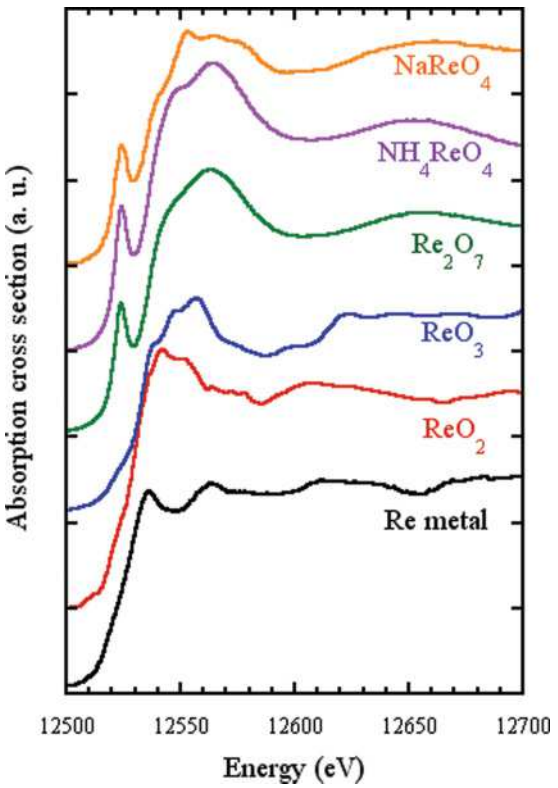

FIG. 1. (Color online) The Re L_1 experimental spectra in the different Re oxides compared with the Re metal. Some show a pre-edge at 12 525 eV, while others just have a shoulder at this energy.

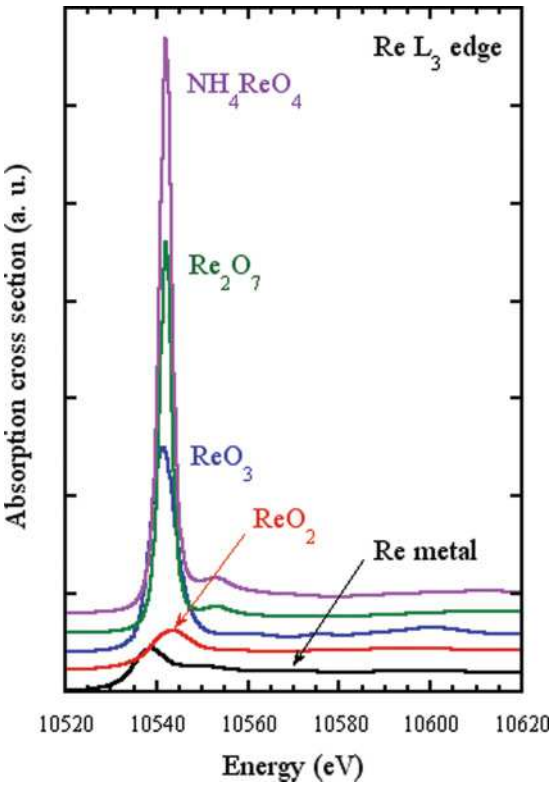

FIG. 2. (Color online) The Re L_3 experimental spectra in the different Re oxides compared with the Re metal. Some show a large white line. The second part of the spectra is flatter than for the L_1 edge but shows secondary features.

The experimental spectra are shown in Figs. 1 and 2 for the L_1 and L_3 rhenium edges, respectively. The L_1 edges show their typical steplike shape. The spectra corresponding to the NH_4ReO_4, $NaReO_4$, and Re_2O_7 compounds present an important pre-edge, at around 12 525 eV, typical of materials with the absorbing atom out of a center of symmetry. For ReO_3, ReO_2, and Re metal, on the contrary, there is only a smooth shoulder at this energy. The L_3 edge spectra are less structured, but have a wide white line, at least for the NH_4ReO_4, ReO_3, and Re_2O_7 compounds. For the others, it can be supposed that the $5d$ orbital is very unlocalized.

IV. THEORY

A. Cross section

The absorption cross section σ normalized with respect to the unit cell has the following expression:

$$\sigma(\omega) = 4\pi^2 \alpha \hbar\omega \sum_j \sum_{f,g} \left|\langle \psi_f | \hat{O} \left| \psi_g^{(j)} \right\rangle\right|^2 \delta\left(\hbar\omega - \left(E_f - E_g^{(j)}\right)\right), \tag{1}$$

where α is the fine-structure constant and $\hbar\omega$ is the photon energy. E_g and E_f are the energies of the ground state $\Psi_g^{(j)}$ and photoexcited state Ψ_f, respectively, with j the index of the atom in the unit cell. The final state Ψ_f is an unoccupied state above the Fermi energy E_F. Ψ_f is calculated assuming an excited electronic configuration of the absorbing atom with a core hole and a complete screening by one electron located in the first unoccupied level. The electron-photon interaction is described classically by means of the electromagnetic operator $\hat{O}$. In the x-ray regime, the magnetic part of the electromagnetic field can be neglected and the remaining electric part is satisfactorily described by the first two terms of the multipolar expansion:

$$\hat{O} = \vec{\epsilon} \cdot \vec{r}\left(1 + \tfrac{1}{2} i \vec{k} \cdot \vec{r}\right), \tag{2}$$

where $\vec{r}$ is the position vector from the absorbing atom, $\vec{\epsilon}$ is the polarization of the photon, and $\vec{k}$ is its corresponding wave vector. The first term of this expansion is responsible for the so-called electric dipole ($E1$-$E1$) transition, whereas the second one induces the electric quadrupole ($E2$-$E2$) one.

B. The calculation code

The *ab initio* simulations of the XANES spectra have been performed using the FDMNES package.[16] In the FDMNES code, the calculations are monoelectronic and carried out in real space, using clusters built around each nonequivalent absorbing atom. As for other monoelectronic approaches, the main difficulty is the calculation of the final states. Two methods are available to calculate the final states: the finite-difference method (FDM) and the multiple-scattering theory (MS). The latter rely on the muffin-tin approximation, which assumes a cluster potential having a spherical symmetry around the atoms and a constant value in the interstitial space.[17]

The FDM is a full potential method that introduces no approximation on the shape of the potential. This makes it an ideal calculation tool for materials in which the nonsphericity plays an important role. The cluster potential is calculated in every point of a thin space grid. Accordingly, the Schrödinger equation is discretized and subsequently solved point by point. Increased CPU time and virtual memory are the price to pay for the gain in accuracy.

FDMNES is *ab initio* in the sense that it generally does not need any auxiliary parameters. Only the atom positions are required and the code starts from the first-principles equations. Nevertheless, in order to gain a better understanding of specific phenomena, it is possible to restrict the values for some specific quantities *a priori*. For example, one can force the calculation with a specific orbital occupancy for a given atom, such as the number of electrons in the $5d$ orbital of the Re absorbing atom. From this initial guess, the Schrödinger (or Dyson) equation is solved and a new set of final states is afforded. At this stage, the important point is that the Fermi level is adjusted in order to match the number of electrons expected for the absorbing atom. In the present paper, all the simulations reported are relativistic.

At the L_1 edge, the core hole is taken into account using the *final-state rule*, i.e., that photoelectron states are obtained with a potential calculated with a hole in the $2s$ level and an extra electron in the first nonoccupied atomic orbital. In contrast, at the L_3 edge, comparisons show that better agreement is obtained when calculating the potential with a nonexcited absorbing atom. Going beyond these rules would require multielectronic and multiatomic simulations that are not trackable in these systems and probably not necessary. To put it more simply, to take into account the core-hole lifetime and other multielectronic phenomena occurring in the absorption process, a convolution procedure was applied to all calculated spectra in this work. At the Fermi level, the Lorentzian width is due to the interaction with the core hole and is equal to 6 eV at the Re L_1 edge and to 4 eV at the Re L_3 edge.[18] For higher photoelectron energy, the collective interactions of the plasmons increase the Lorentzian width up to 7 eV.

V. RESULTS AND DISCUSSION

A. Qualitative analysis

According to the dipolar selection rules, the absorption at the L_3 edge is mainly caused by the transition of the photoelectron from the core level $2p_{3/2}$ to the level nd (with $n = 5$ for rhenium), the transition toward the $6s$ level being quantitatively very small (but not neglected). At this absorption edge, the probed final states are energetically and spatially more localized than at the L_1 edge. This results in a strong transition peak, known as the so-called white line. The width of the white line is related to the strength of the orbital localization and depends a lot on the chemical properties of the absorbing element. When the localization is strong enough, the integrated intensity of the white line is proportional to the number of holes in the corresponding band (ten minus the number of electron in the orbital $5d$). As a consequence, the higher the oxidation state of the compound is, the higher is the white line. In contrast, at the Re L_1 edge, the transition occurs from the $2s$ states, and the final states, mainly the $6p$, are delocalized so that there is no clear white line. Nevertheless, the Re $6p$

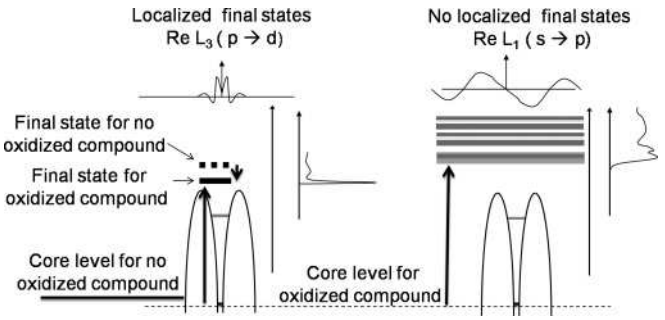

FIG. 3. Consequence of the oxidation process on XANES shift energy. Left: for localized final states, both the core level and the final states are shifted downward under oxidation, and no or a very small shift of the spectra is observed. Right: the nonlocalized final states are almost not shifted downward in the oxidation process, in contrast with the core levels. This leads to a shift of the XANES spectra toward higher photon energy.

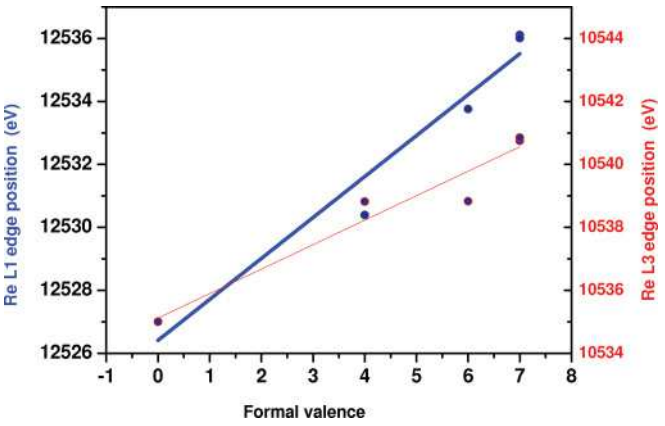

FIG. 4. (Color online) Position of the experimental spectra in the different Re oxides compared with the Re metal. The edge position is set at the maximum of the first derivative.

orbital is highly hybridized with the surrounding environment, making the L_1 edge extremely sensitive to the local geometry. Therefore, the third and sometimes even higher shells can be assessed not only on the first shell around the absorbing atom, but also on the second one. This results in a long-distance sensitivity on the geometrical structure, typically up to 4 or 5 Å from the absorbing atom. The L_1 edge, as the K edge, can also be a probe for the oxidation state of the absorbing atom, but in another way. Indeed, a global shift of the XANES spectra toward higher energy is observed when the oxidation state increases. This can be explained by the fact that under oxidation, the core level becomes more bounded and its energy level is thus lower. On the other hand, the final unlocalized states are almost not shifted (see Fig. 3), so that the energy gap needed for the transition is higher. Concerning the L_3 edge, this phenomenon is less pronounced as the energy of the final localized $5d$ states is shifted downward together with that of the core level. In the case of the $3d$ elements, the $3d$ states are much more localized than the corresponding $5d$ states of the rare earth. Consequently, the phenomenon described above is stronger (the $3d$ states shift rather strongly under oxidation, as do the core state) and thus the L_{23} edges shift very little in comparison with the K edges.

These considerations are in agreement with our measurements. In Fig. 4, we show the relative shifts of the edges versus the reference Re metal sample. Note that the choice of the edge position is rather arbitrary, especially when the edge shapes (and thus the structures of the different samples) are very different, as in our case. In any event, we choose for the edge position the maximum of the first derivative. In this way, but probably with a large degree of uncertainty, we found a clear correlation between the formal oxidation state of the Re atom and the edge shift. We found also that this shift is wider in the L_1 case than in the L_3 case.

B. Simulations

In Figs. 5 and 6, we show the final agreement between the simulations and the experiments. It can be seen than this agreement is rather good except for the white line amplitude in the L_3 edges. This fact will be discussed in the next section, but already note that we chose to match the spectra intensity in the flat part after the white lines. All the main structures, but also most of the secondary ones, are reproduced by the simulation.

Different radii were used for the simulations to check convergence. We found that this was reached using a 4 Å radius for both edges, but in the L_1 edges in ReO_3 a 6 Å radius appeared to be necessary. Simulations were done, in most cases, using the finite-difference method. Indeed, we found that often the muffin-tin approximation was not able to give a satisfactory agreement. For example, in Fig. 7 we compare both simulation techniques in the ReO_3 L_1 case. The agreement is clearly less good with the MST in the lower energy part of the spectra. It can be checked that at the L_3 edge, when the white line is not well reproduced, the secondary structures at higher energy are nevertheless given by the simulation, relatively well in amplitude. See, for example, the peak between 10 522 and 10 525 eV in all the compounds and also the inset in the figure corresponding to the ReO_3 case. We should also mention that Re_2O_7 is a peculiar case because its unit cell contains four nonequivalent Re atom sites, all in the $C1$ symmetry. The resulting spectrum is thus the sum of the contributions from all these sites. Moreover, the $C1$ symmetry makes the simulation especially heavy in term of computing time when using the FDM approach, and only MST simulations are presented in this case. We have checked that the pre-edge is stronger for the two tetrahedral sites than for the octahedral ones. In spite of the fact that these are rather strongly distorted (thus losing also their center of symmetry), they also show a pre-edge.

C. Sensitivity on the structure

At the rising L_1 edge, a significant pre-edge is observed in three of the experimental spectra. They are reproduced by the simulation. The pre-edge is caused by the dipolar $2s \rightarrow 6p$ transition, similar to the main edge. We verified that the quadrupolar transition is negligible for all the compounds. This peak is a typical signature of noncentrosymmetric sites. Indeed, at this photoelectron energy we find the $5d$ states, which are not accessible according to the dipolar selection rules for the L_1 absorption edge. The absence of a center

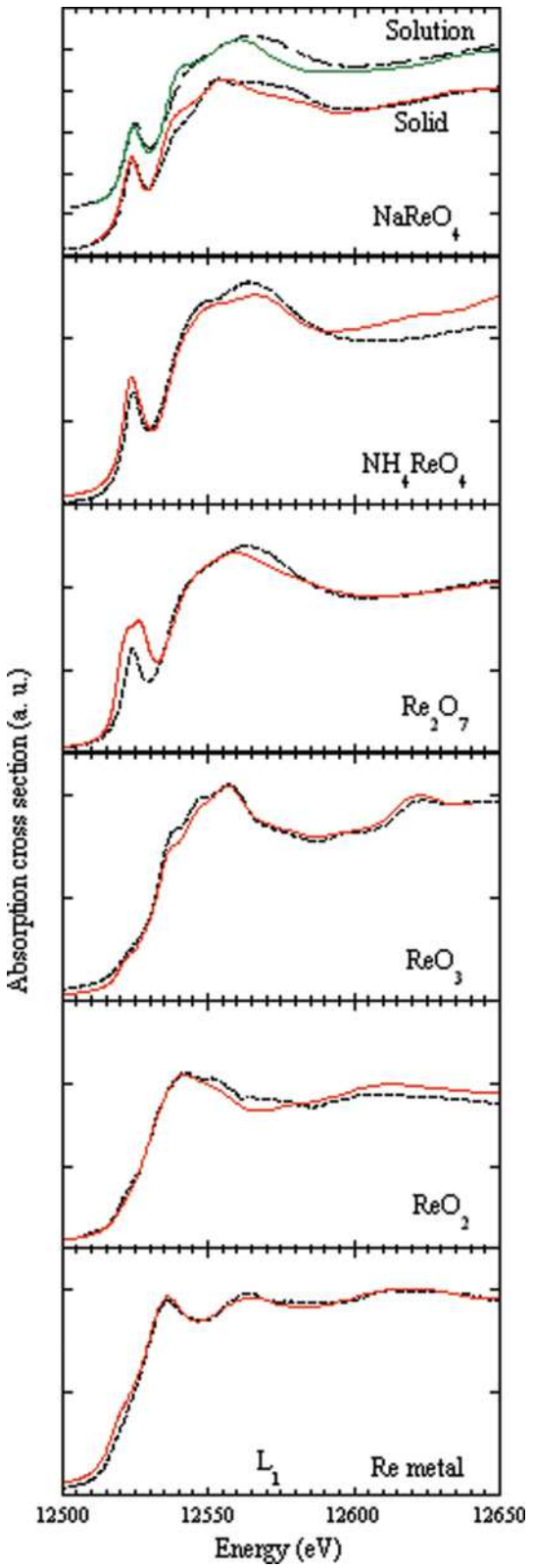

FIG. 5. (Color online) The Re L_1 experimental and calculated XANES spectra in the different compounds. Dotted, experiment. Full line, simulations using the FDM approaches for all the oxides but for Re_2O_7 where MST is used. The simulation is able to give all the experimental structures. For $NaReO_4$, the experimental spectra for the sample in solution is also shown shifted up with a simulation with a 2 Å cluster radius.

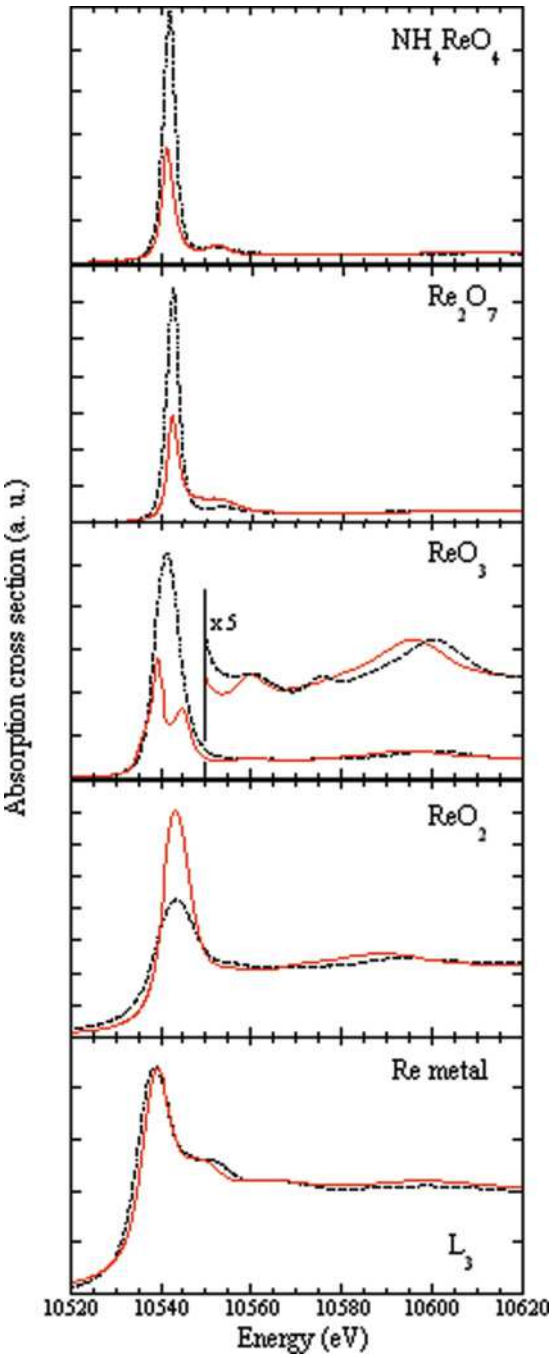

FIG. 6. (Color online) The Re L_3 experimental and calculated XANES spectra in the different compounds. Dotted, experiment. Full line, simulations using the FDM approaches for all the oxides but for Re_2O_3 where MST is used. The simulation is able to give most experimental structures. The white line amplitude is not well reproduced specially for ReO_3, but the secondary features are there.

of symmetry makes the odd-even hybridization between the $6p$ and $5d$ orbitals possible. This leads to a relatively strong densityof p states at this energy. The agreement on this feature is less good for Re_2O_7. We first recall that this compound is the only one calculated under the muffin-tin MST technique. Considering the general quality of the agreement between experiments and theory for the L_1 edges, we do not think that that this fact completely explains the discrepancy.

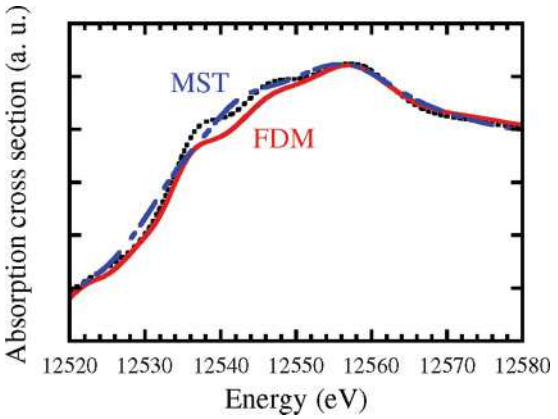

FIG. 7. (Color online) The Re L_1 experimental and calculated XANES spectra in ReO_3. Dotted line, experiment; full line, simulations using the FDM approaches; mixed line, simulation using the MST under the muffin-tin approximation. The three bumps in the rising edge are reproduced only using the full potential approach.

A complementary explanation for this difference could be related to the chemical evolution of the compound to its hydrated form ($HReO_4$), in which the Re atom symmetry is purely tetrahedral,[19] during the acquisition of the experimental spectrum. We can thus assume that the acquired experimental spectrum could contain, in addition to the dehydrated Re_2O_7 compound, a proportion of $HReO_4$.

In the simulations, the cluster size was a decisive parameter to achieve good agreement with experiment. This was true for all the series and more specifically at the L_1 edge. We already mentioned the necessity to go up to 6 Å to reach a good agreement for ReO_3. This result is interesting since it gives a possible signature of the minimum size and the relative "crystallinity" of clusters formed on surfaces of supported catalysts. In catalysis, the size of the clusters is generally determined by x-ray diffraction. We show here that XANES can be an alternative to this method, especially when considering very small clusters. In the same way, simulation with a 2 Å radius in NH_4ReO_4 makes the peak at 12 550 eV almost not visible. This is due to the second neighboring tetrahedron standing between 2 and 4 Å from the absorbing Re. This is in agreement with theoretical results already reported by Garcia *et al.* at the Mn *K* edge absorption spectrum of $KMnO_4$ solution.[20] This is also in good agreement with the experimental results obtained by Froba *et al.*[21] at the Re L_1 absorption edge in $HReO_4$. The authors observed a second peak only for the spectra recorded in the solid state. In the XANES spectrum of the salt in aqueous solution, the second peak vanishes. They explained this as being due to the loss of the tridimensional long-range order when changing from a solid state to a solvated liquid state.

Another example to illustrate the sensitivity on the order at longer range is the comparison between NH_4ReO_4 and $NaReO_4$. In spite of the fact that the solid-state structures of these compounds are supposed to be similar (both are made up of isolated ReO_4 units), the XANES spectra look slightly different. More precisely, a marked feature at around 12 551 eV that is particular to the spectrum of $NaReO_4$ in the solid state (Fig. 5) is observed that was not present in the spectrum of

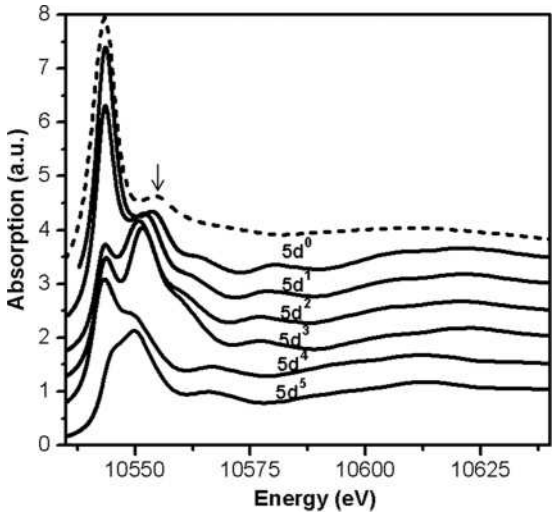

FIG. 8. The Re L_3 experimental and MS calculated XANES spectra in NH_4ReO_4 at the solid state. Dotted line, experiment; full line, simulation for different orbital occupancy. The simulations are shifted in order to align the main peak with experiment.

NH_4ReO_4. The simulation reproduces it when performed for a cluster-size calculation radius higher than 3 Å. Such a value corresponds to the distance between the absorbing Re atom and the second oxygen shell neighbor. The distances between the Re atom and the second oxygen shell are different between both compounds, i.e., 3.06 and 3.30 Å, respectively. This difference was not detected using extended x-ray-absorption fine-structure (EXAFS) analysis. Indeed, even if EXAFS is supposed to be sensitive to the distance variation of 0.02 Å, its sensitivity decreases dramatically when the second shell is only composed of light atoms. As already reported by Ravel,[22] the present study shows again that XANES can be very sensitive to the position of such light atoms. Thus, this low-range photoelectron energy technique is highly relevant to establishing the existence of a second shell which cannot be detected by EXAFS. Another point supporting all this is the difference observed between the $NaReO_4$ spectra recorded in an aqueous solution and in solid phase (see Fig. 5). The amplitude of the second peak is weaker in the case of the measurement in the aqueous solution. This is easily explained by the loss of long-range order when moving from the solid to the aqueous state. The experimental spectrum recorded in the aqueous solution then becomes closer to the calculation with a cluster radius equal to 2 Å, which thus contains only one Re and its first oxygen ligands.

D. Sensitivity on the oxidation state

We did simulations imposing different oxidation states for each compound. As expected, the L_3 edge is more sensitive than the L_1 one because the white line amplitude depends directly on the 5*d* occupation number. See, for example, the variation in the case of NH_4ReO_4 shown in Fig. 8. The agreement with experiment is clearly better with a low occupancy rate. In this figure, we choose to align the white line for clarity, but a shift of the calculated spectra also occurs with the oxidation state. As stated above, this is due to the concomitant shifts of final and initial states. Because

our procedure is rather crude, we do not expect a perfect reproduction of the experimental shift, but we do expect at least a good trend, in agreement with what can be expected using a fit only on the spectra shape. We also observe that the position of the second peak for most compounds depends on the oxidation state of the Re atom as well. This underlines the fact that the white line amplitude is not the only feature that is sensitive to the oxidation state.

We found the best agreement with a $5d^0$ configuration for Re_2O_7, $5d^1$ for NH_4ReO_4 and $NaReO_4$, and $5d^5$ for ReO_2 and ReO_3, with all of these values applying to both the L_1 and L_3 spectra. There is thus a large difference with the formal value expected for ReO_2 and ReO_3, where $5d^3$ and $5d^1$ configurations are expected. The calculated shift follows the same trend but overestimates the experimental value in the case of Re_2O_7 (we artificially shifted the calculated spectra in Figs. 5 and 6 for this compound to match the experiment). In contrast with the other compounds calculated using the FDM, in this case we had the difficulty coming from the muffin-tin approximation and especially of the interstitial potential definition inherent to this approximation. The good point in these results is that the L_1 and L_3 fits are coherent. However, there remains a huge difference between the formal occupancy number in ReO_3 and the one calculated. It should be noted that there is very good agreement in the L_1 spectra shape. These spectra are also slightly sensitive to the orbital occupancy, showing a better agreement with the $5d^5$ occupancy rate. It is also for this compound that we obtain the agreement at the white line in the L_3 edge. We have no definite explanation for this anomaly. However, in the series, this specific compound is special in the sense that it is the only one that is metallic, all the others being insulating.[23,24] It was not possible to take this aspect into consideration in the present study. Another possible explication might be found in some of the nonunderstood multielectronic effects. In any case, the formal occupation number is an ionic picture that is probably not adaptable to a metallic material. Moreover, for the $5d$ orbitals, which have a rather large radius and thus overlap strongly the neighboring atoms (far more at least that the $3d$ orbital of the $3d$ transition elements), the atomic charge included in the atomic radius certainly does not correspond with the formal charge. In this context, a more detailed description of the electronic structure resulting from a self-consistent and full-potential calculation could in an *ab initio* way make the leap between the formal occupancy rate and the real charge into the atomic radius and thus with the edge shifts. This is beyond the scope of the present study.

VI. CONCLUSION

We have compared theoretical and experimental XANES spectra in a series of Re oxides. We showed how powerful the approach is of combining the use of two absorption edges, L_1 and L_3, to obtain additional information and more confidence in the results. L_1 is indicative of the geometrical structure, whereas the L_3 edge gives an estimation of the oxidation state. The FDM is well suited to simulate these kinds of structures and to give insights into the relevant parameters influencing the edge features at both edges. In some cases, the MS is sufficient to reproduce the experimental resonances. Taking into account the overall conclusions arising from this deep investigation of rhenium reference compounds, we are now confident in the next step, which will be the study of the supported Re catalysts.

ACKNOWLEDGMENTS

We wish to acknowledge the Agence Nationale de la Recherche for funding under Contract No. ANR-07-BLAN-0265-01: Spectroscopie d'Absorption X Operando (SAXO). Some of the numerical results presented in this paper were carried out using the regional computational cluster supported by Université Lille 1, CPER Nord-Pas-de-Calais/FEDER, France Grille, and CNRS. We greatly appreciate and thank the technical staff of the CRI-Lille 1 center for their strong and helpful support.

[1] J. C. Mol, Catal. Today **51**, 289 (1999).
[2] Y. Yuan and Y. Iwasawa, J. Phys. Chem. B **106**, 4441 (2002).
[3] J. Gornay, X. Secordel, G. Tesquet, B. de Menorval, S. Cristol, P. Fongarland, M. Capron, L. Duhamel, E. Payen, J.-L. Dubois *et al.*, Green Chem. **12**, 1722 (2010).
[4] B. Mitra, X. Gao, I. E. Wachs, A. M. Hirt, and G. Deo, PhysChemChemPhys. **3**, 1144 (2001).
[5] X. Scordel, E. Berrier, M. Capron, S. Cristol, J.-F. Paul, M. Fournier, and E. Payen, Catal. Today **155**, 177 (2010).
[6] R. J. Lobo-Lapidus, M. J. McCall, M. Lanuza, S. Tonnesen, S. R. Bare, and B. C. Gates, J. Phys. Chem. C **112**, 3383 (2008).
[7] A. Yoboué, A. Susset, A. Tougerti, D. Gallego, S. Venkat Ramani, M. Kalyanikar, D. S. Dolzhnikov, S. G. Wubshet, Y. Wang, S. Cristol *et al.*, Chem. Commun. **47**, 4285 (2011).
[8] H. S. Lacheen, P. J. Cordeiro, and E. Iglesia, J. Am. Chem. Soc. **128**, 15082 (2006).
[9] S. R. Bare, S. D. Kelly, B. Ravel, N. Lay, L. King, and G. E. Mickelson, PhysChemChemPhys **12**, 7702 (2010).
[10] Y. Joly, *New Trends Series: Springer Proceedings in Physics* (Springer, Berlin, 2010), Vol. 133, Chap. 3, pp. 77–125.
[11] A. Atzersdorfer and K. Range, Z. Naturforsch., B **50**, 1417 (1995).
[12] A. Magnéli, Acta Chem. Scand. **11**, 28 (1957).
[13] J.-E. Jorgensen, J. D. Jorgensen, B. Batlogg, J. P. Remeika, and J. D. Axe, Phys. Rev. B **33**, 4793 (1986).
[14] B. Krebs, A. Mueller, and H. H. Beyer, Inorg. Chem. **8**, 436 (1969).
[15] V. Briois, E. Fonda, S. Belin, L. Barthe, M. Rubbens, F. Villain, and C. La Fontaine, Proceedings of UVX 2010 - 10e Colloque sur les Sources Cohérentes et Incohérentes UV, VUV et X; Applications

et Développements Récents, UVX 2010, EDP Science (2011), pp. 41–47.
[16]Y. Joly, Phys. Rev. B **63**, 125120 (2001).
[17]J. J. Rehr and R. C. Albers, Rev. Mod. Phys. **72**, 621 (2000).
[18]M. O. Krause and J. H. Olivier, J. Phys. Chem. **8**, 329 (1979).
[19]G. Wltschek, I. Svoboda, and H. Fuess, Z. Anorg. Allg. Chem. **619**, 1679 (1993).
[20]J. Garcia, M. Benfatto, C. Natoli, A. Bianconi, I. Davoli, and A. Marcelli, Solid State Commun. **58**, 595 (1986).
[21]M. Froba, K. Lotche, and W. Metz, J. Phys. Chem. Solids **57**, 635 (1996).
[22]B. Ravel, J. Alloys Compd. **401**, 118 (2005).
[23]F. Cora, M. G. Stachiotti, C. R. A. Catlow, and C. O. Rodriguez, J. Phys. Chem. B **101**, 3945 (1997).
[24]R. A. Evarestov, A. Kalinko, A. Kuzmin, M. Losev, and J. Purans, Integr. Ferroelectr. **108**, 1 (2009).